Diabetologia (2012) 55:835–844
DOI 10.1007/s00125-011-2416-x

ARTICLE

Disruption of the association of integrin-associated protein (IAP) with tyrosine phosphatase non-receptor type substrate-1 (SHPS)-1 inhibits pathophysiological changes in retinal endothelial function in a rat model of diabetes

L. A. Maile · K. Gollahon · C. Wai · G. Byfield · M. E. Hartnett · D. Clemmons

Received: 1 July 2011 / Accepted: 24 November 2011 / Published online: 23 December 2011

Abstract
Aims/hypothesis We have previously shown that the association of integrin-associated protein (IAP) with tyrosine phosphatase non-receptor type substrate-1 (SHPS-1) regulates the response of cells, including osteoclasts, osteoblasts, smooth muscle and retinal endothelial cells, to IGF-I. Here we sought to: (1) determine whether the regulation of IGF-I responsiveness by the association of IAP with SHPS-1 is a generalised response of endothelial cells; (2) identify the mechanism by which this association contributes to changes in endothelial cell responses to IGF-I; and (3) determine whether inhibition of this association alters pathophysiological changes occurring in vivo.
Methods Endothelial cells were maintained in 5 mmol/l glucose and at hyperglycaemic levels, and exposed to an anti-IAP antibody that disrupts the association between IAP and SHPS-1. A rodent model of diabetes with endothelial cell dysfunction was used to investigate the role of the association of IAP with SHPS-1 in endothelial cell function in vivo.
Results Endothelial cells maintained in 5 mmol/l glucose showed constitutive cleavage of the extracellular domain of IAP (which contains the SHPS-1 binding site), with no association between IAP and SHPS-1 being detected. In contrast, hyperglycaemia inhibited IAP cleavage, allowing IAP to associate with SHPS-1 and IGF-I to stimulate SHPS-1 tyrosine phosphorylation. Exposure to the anti-IAP antibody inhibited IGF-I-stimulated tube formation and increased permeability. In the rodent model, basal IAP–SHPS-1 association was not detected in retinal extracts from normal rats, but was fully restored in rats with diabetes. The anti-IAP antibody inhibited the association of IAP with SHPS-1, and reduced retinal vascular permeability and leucocyte adherence to levels similar to those in non-diabetic rats. The antibody also significantly inhibited the aberrant neovascularisation induced by hypoxia.
Conclusions/interpretation Our results demonstrate that the increased association of IAP with SHPS-1 contributes to the pathophysiological changes in the endothelium that are induced by hyperglycaemia and hypoxia.

Keywords Diabetic retinopathy · Hyperglycaemia · Hypoxia · Insulin-like growth factor I · Integrin-associated protein · Neovascularisation · Occluding · Vascular permeability

Abbreviations

c-SRC	Proto-oncogene Src
IAP	Integrin-associated protein
IVNV	Intravitreal neovascularisation
p	Postnatal day
REC	Retinal endothelial cell
ROP	Retinopathy of prematurity

L. A. Maile · K. Gollahon · C. Wai · G. Byfield · D. Clemmons
Departments of Medicine and Ophthalmology,
School of Medicine, University of North Carolina at Chapel Hill,
Chapel Hill, NC, USA

M. E. Hartnett
Department of Ophthalmology,
University of Utah School of Medicine,
Salt Lake City, UT, USA

L. A. Maile (✉)
CB# 7170, 5029 Burnett Womack, Division of Endocrinology,
University of North Carolina,
Chapel Hill, NC 27599-7170, USA
e-mail: laura_maile@med.unc.edu

SHPS-1	Tyrosine phosphatase non-receptor type substrate-1
VE cadherin	Vascular endothelial cadherin
VEGF	Vascular endothelial growth factor
ZO1	Zonula occludens protein 1

Introduction

Changes in endothelial cell function in response to hyperglycaemia include increased vascular permeability and increased leucostasis, as well as increased cellular proliferation leading to new blood vessel formation. The enhanced responsiveness of vascular cells to IGF-I has been implicated in all these vascular responses to hyperglycaemia. Hypophysectomy decreases serum IGF-I concentrations and arrests retinopathy progression [1]. IGF-I levels in vitreous correlate with the presence of proliferative retinopathy [2] and the administration of somatostatin analogues, which decrease IGF-I levels in vitreous, slows retinopathy progression [3]. Mice that overproduce IGF-I in the retina develop changes associated with diabetic retinopathy, including increased capillary permeability and angiogenesis [4].

The biological responses of smooth muscle and retinal endothelial cells (RECs) to IGF-I are enhanced when cells are cultured in hyperglycaemic conditions [5, 6]. This response is dependent upon the hyperglycaemia-facilitated association of two cell surface proteins, integrin-associated protein (IAP, also known as CD47) and. tyrosine phosphatase non-receptor type substrate-1 (SHPS-1) [5, 7, 8]. The aims of this current study were: (1) to determine whether the regulation of IGF-I responsiveness by the association of IAP with SHPS-1 is a generalised response of endothelial cells to hyperglycaemic conditions; (2) to identify the mechanisms by which the association between IAP and SHPS-1 contributes to hyperglycaemia-mediated changes in endothelial cell responses to IGF-I; and (3) to determine whether inhibition of that association alters the pathophysiological changes that occur in vivo in rodent models of retinopathy.

Methods

Endothelial cell culture Primary HUVECs (Lonza, Walkersville, MD, USA) were grown in M-199 (Life Technologies, Grand Island, NY, USA) plus EGM-2 Endothelial Cell Growth Medium supplements (Lonza) containing 5 mmol/l glucose. HUVECs were switched to growth medium containing 15 mmol/l glucose for 3 days. Mannitol (10 mmol/l) was added to the medium containing 5 mmol/l glucose to control for the difference in osmolarity. Cultures were quiesced for 14 h in serum-free M-199 containing 5 or 15 mmol/l glucose, and exposed to IGF-I (50 ng/ml; Genentech, San Francisco, CA, USA), the monoclonal anti-IAP antibody, B6H12 (1 μg/ml), as described previously [8], or the vascular endothelial growth factor (VEGF) inhibitor Je-11 (10 μg/ml) (EMD Biosciences, Rockland, MA, USA). RECs were grown as described previously [5]. The use of human cells was approved by the University of North Carolina Ethics Committee.

Cell lysis, immunoprecipitation and immunoblotting Lysates were immunoprecipitated, separated by SDS-PAGE and transferred to Immobilon filters (Millipore, Billerica, MA, USA) prior to immunoblotting to visualise proteins [5]. Antibodies used for immunoblotting were anti-phosphotyrosine (PY99; Santa Cruz, Santa Cruz, CA, USA), anti-SHPS-1 (BD Biosciences, Franklin Lakes, NC, USA), anti-occludin (Invitrogen, Carlsbad, CA, USA) and anti-VEGF R2 (R&D Systems, Minneapolis, MN, USA).

Real-time PCR analysis of VEGF mRNA Total RNA was collected using a kit (RNAeasy kit; Qiagen, Valencia, CA, USA). cDNA was made using 1 μg RNA and a high-capacity cDNA reverse transcription kit (Life Technologies). Real-time PCR reactions were set up using the TaqMan gene assay kit and primer probe sets (for *VEGFA* Hs0090005_ml, for *GAPDH* Hs 999999905_ml; ABI, Carlsbad, CA, USA). Reactions were performed in quadruplicate. ABI SDS 2.2.2 software was used to determine relative amounts of RNA.

In vitro vascular permeability assay HUVECs were plated in growth medium (15 mmol/l glucose) on collagen-coated Transwell inserts (24 well). After 24 h, the medium was changed to SFM-199 (15 mmol/l glucose), which contained IGF-I (50 ng/ml) plus B6H12 (1 μg/ml). After 14 h, fluorescently labelled dextran (0.5 mg/ml, average molecular mass 70 kDa; Sigma, St Louis, MO, USA) was added. After 1 h, the medium was collected from the lower chamber and the amount of FITC-dextran was measured in a fluorescence-detecting microplate reader (Fluor Imager 595; Molecular Dynamics, Sunnyvale, CA, USA), with excitation and emission wavelengths of 294 and 521 nm respectively.

In vitro tube formation assay HUVECs maintained in 15 mmol/l glucose were switched to SFM-199 containing IGF-I (50 ng/ml) and B6H12 (1 μg/ml) for 14 h. They were then plated on 24-well plates coated with 500 μl growth factor-reduced Matrigel (1.5×10^5 cells/ml per well; BD Biosciences). After 4 h, the plates were photographed at magnification ×10 and the number of tubes per square centimetre in six random areas of each well was determined [9]. One tube was considered to be between two branch points.

In vitro measurement of leucocyte adhesion RECS were plated in 96-well plates (3×10^4 cells/100 μl per well) in

growth medium (15 mmol/l glucose). After 48 to 72 h, SFM-199 (15 mmol/l glucose) was added for 4 h, with or without TNFα (30 ng/ml; Life Technologies) for 2 h. The monolayer was rinsed three times, then 100 μl labelled leucocytes was added. The monolayers were again rinsed three times and 100 μl/ml SFM-199 was added prior to visualisation with a fluorescence microscope (Leica, Weztlar, Germany; excitation and emission wavelengths 485 and 530 nm respectively). Adherent, fluorescent leucocytes were counted.

Preparation of HL-60 leucocytes Leucocytes (1×10^6) were incubated for 1 h at 37°C with 1 μg/ml Calcein-AM (BD Biosciences) in SFM-199 (15 mm/l glucose). The labelled cells were then loaded on to the REC monolayer (100 μl/well) and 500 μl SFM-199 was added to the lower chamber.

Animals for diabetes study Male Sprague–Dawley rats (Charles River, Wilmington, MA, USA) were housed under 12–12 h light–dark conditions, with free access to food and water. All protocols were approved by the University of North Carolina at Chapel Hill Animal Care and Use Committee, and adhere to the National Institutes of Health guidelines and to the Association for Research in Vision and Ophthalmology Statement for the Use of Animals in Ophthalmic and Visual Research.

Diabetes induction protocol Control rats received an injection of vehicle. Streptozotocin was given by intraperitoneal injection (50 mg/kg body weight). Hyperglycaemia was confirmed 6 days later. At that point insulin injections were commenced (9 U/kg daily; NPH insulin, Novo Nordisk, Princeton, NJ, USA). At 20 days post-injection, ten animals in the streptozotocin group received an injection of control mouse IgG (50 μg/kg) and ten received an injection of B6H12 (50 μg/kg) every 72 h for 30 days. Further details are given in Table 1.

In vivo measurement of vascular permeability Rats were injected with pentobarbital (80 mg/kg body weight) (Southern Anesthesia, West Columbia, SC, USA). Once deep anaesthesia had been achieved, warmed Evans Blue (45 mg/kg; Fisher Scientific, Pittsburgh, PA, USA) was injected into the tail vein. Evans Blue dye binds to albumin, allowing the measurement of albumin leakage from the vasculature [10]. After 2 h, a lethal dose of anaesthetic (100 mg/kg) was administered. Blood was collected and centrifuged at 12,000×*g* for 5 min. The rats were perfused with 1% (wt/vol.) paraformaldehyde in citrate, then the eyes were removed and placed in PBS. The retinas were removed, lyophilised, then resuspended in formamide and incubated at 70°C. After 18 h the retinas with formamide were centrifuged at 13,000×*g* for 10 min.

A standard curve was generated using serial dilutions of Evans Blue (30 mg/μl). The absorbance was measured using a Nanodrop spectrophotometer (Thermoscientific, Rockford, IL, USA) with excitation and emission wavelengths of 620 and 740 nm respectively. The amount of Evans Blue permeation from each retina was calculated as follows: (Evans Blue [μg]/retina dry weight [g])/(time−averaged Evans Blue concentration [μg]/plasma [μl]×circulation [h]).

In vivo measurement of leucocyte adhesion Rats were anesthetised with pentobarbital as above. The chest cavity was opened, and a 19 gauge needle inserted into the left ventricle and infused with PBS (300 ml/kg), followed by 1% paraformaldehyde (100 ml/kg), 1% (wt/vol.) BSA in PBS (20 ml/kg), concanavalin A FITC (Vector Labs, Burlingame, CA, USA) at a concentration of 40 mg/ml in PBS (5 ml/kg) and finally PBS (20 ml/kg). Blood was collected and the eyes removed and placed in paraformaldehyde. After 2 h, the eyes were rinsed twice in PBS. Retinas were isolated, and the hyaloidal vessels and vitreous removed with ora serratas intact. By making four incisions 90° apart, the retinas were flattened and then mounted on to microscope slides.

Analysis of retinal homogenates Retina were removed from the eye, frozen in modified radioimmunoprecipitation assay buffer with a protease inhibitor cocktail (HALT; Thermoscientific) and analysed by immunoblotting [5].

Rodent model of retinopathy of prematurity On postnatal day (p) 0, litters of 12 to 14 newborn Sprague–Dawley rat pups with their mothers (Charles River) were placed in an incubator (OxyCycler; BioSpherix, New York, NY, USA) and inspired oxygen cycled between 50% and 10% every 24 h. From p12, rat pups were given a daily intraperitoneal injection of B6H12 (20 μg per pup) or control IgG for 6 days. After seven cycles of oxygen fluctuations at p14, pups were placed in room air for 4 days. Oxygen and carbon dioxide levels were monitored daily [11].

After these animals were killed at p18, their eyes were fixed in paraformaldehyde 2% (wt/vol.). Retinas were isolated with ora serratas intact and placed in PBS. Four

Table 1 Characteristics of the streptozotocin-induced rat model of hyperglycaemia

Rat group	Weight (g)[a]	Glucose (mmol/l)	Diabetes duration (days)
Control	333±23	8.14±0.5	–
Diabetic	306±7	25±0.9*	50
Diabetic+B6H12	276±7	23.2±0.95*	50

Data are mean±SEM, $n>20$

*$p<0.05$ compared with control group

[a] The rate of weight gain was attenuated in the diabetic group, but no rat lost weight

incisions 90° apart were made, and the retinas flattened and mounted on to slides [12].

To stain the vasculature, the flattened retinas were permeabilised in 70% ethanol, and then placed in PBS and 1% (vol./vol.) Triton X-100, followed by incubation with Alexa Fluor 568-conjugated *Griffonia simplicifolia* (Bandeiraea) isolectin B4 (5 μg/ml) (Invitrogen) [13]. Images of the retinal blood vessels were captured using a research upright microscope (Nikon 80i; Nikon, Melville, NY, USA) with Surveyor/TurboScan software (Nikon), and digitally stored for analysis.

Total retinal area, summed peripheral avascular retinal area and areas of intravitreal neovascularisation (IVNV) were computed in pixels using Image Tool version 3 (The Dental School, University of Texas, San Antonio, TX, USA) and converted to mm^2 (using a calibration bar). The IVNV was defined as neovascularisation growing into the vitreous at the junction of vascular and avascular retina [14]. For clock hours, flat mounts were divided into 12 clock hours of equal area using Adobe Photoshop (Adobe Systems, San Jose, CA, USA) and the number of clock hours (0–12) exhibiting IVNV determined [15, 16]. Areas of neovascularisation were measured, summed and expressed as a percentage of total retinal area. Measurements were performed by two independent masked reviewers.

Protein estimation The protein concentration of lysates was determined using a BCA protein assay kit (Thermoscientific).

Statistical analysis Chemiluminescent images were obtained from autoradiographs (Thermoscientific) and analysed as described [5]. The Student's *t* test was used to compare differences between treatments. The results shown are representative of at least three independent experiments.

Results

Regulation of the association of IAP with SHPS-1 in vitro To determine whether the hyperglycaemia-induced increase in IAP–SHPS-1 association was a more generalised response of endothelial cells to glucose, we examined the association of IAP with SHPS-1 in HUVECs. Consistent with our previous observations in RECs [5], we found a significant fivefold (±0.9) (mean±SEM; $n=3$) increase in the association of IAP with SHPS-1 when HUVECs were cultured in 15 compared with 5 mmol/l glucose (Fig. 1a). This was associated with a 24±7-fold (mean±SEM; $n=3$) increase in SHPS-1 phosphorylation in response to IGF-I (Fig. 1b), which is comparable to our previous data in RECs [5]. The lack of IAP–SHPS-1 association in vascular smooth muscle cells maintained in 5 mmol/l glucose is due to cleavage of the extracellular domain of IAP, the region of IAP that contains the SHPS-1 binding site [7]. Immunoblotting of lysates from HUVECs and RECs with the anti-IAP antibody (B6H12), which detects intact IAP and the residual membrane-associated fragment that is present after cleavage, revealed that IAP was degraded in 5 mmol/l glucose (Fig. 1c).

Disruption of the association of IAP with SHPS-1 blocks IGF-I-stimulated increases in endothelial cell permeability We next determined whether the glucose-mediated increase in IAP–SHPS-1 association played a role in the regulation of endothelial permeability in response to hyperglycaemia and IGF-I. IGF-I stimulated a significant 2.4±0.14 (mean±SEM; $n=3$, $p<0.01$) increase in the amount of dextran permeating the HUVEC monolayer in 1 h. However, when cells were incubated with B6H12, which disrupted the IAP–SHPS-1 association, no significant increase in dextran permeation was seen, compared with control (Fig. 2a).

A decrease in the junction protein occludin has been implicated in vascular permeability in diabetes. In HUVECs and RECs cultured in 15 mmol/l glucose, IGF-I stimulated a significant decrease in occludin levels (by 5.3±1.2- and 7.5±1.9-fold respectively, mean±SEM; $n=3$, $p<0.01$). The decrease was completely blocked by co-incubation with B6H12 (Fig. 2b).

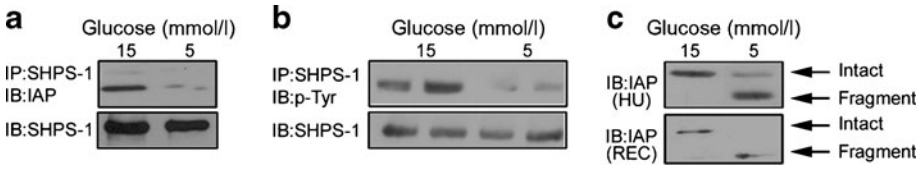

Fig. 1 Glucose regulation of IAP cleavage and the association of IAP with SHPS-1. HUVECs and RECs were grown to confluency in 15 or 5 mmol/l glucose, prior to overnight incubation in serum-free medium with the appropriate glucose concentration. **a** The association of IAP with SHPS-1 was determined by immunoprecipitating (IP) HUVEC lysates using an anti-SHPS-1 antibody, then immunoblotting (IB) with an IAP antibody (B6H12). Equal amounts of protein were separated by SDS-PAGE and immunoblotted with the anti-SHPS-1 antibody to demonstrate that the difference in the association of IAP with SHPS-1 was not due to differing SHPS-1 levels. **b** Cell lysates were obtained from HUVECs that had been exposed to IGF-I (50 ng/ml) for 5 min. The lysates were immunoprecipitated with an anti-SHPS-1 antibody and immunoblotted for phosphotyrosine (p-Tyr). To control for loading, an equal amount of lysate was immunoblotted for SHPS-1. Bands shown are from discontinuous lanes of the same gel. **c** To examine IAP cleavage, equal amounts of HUVEC (HU) and REC lysate were separated by SDS-PAGE and immunoblotted with the anti-IAP antibody B6H12, which recognises intact IAP and fragments of IAP

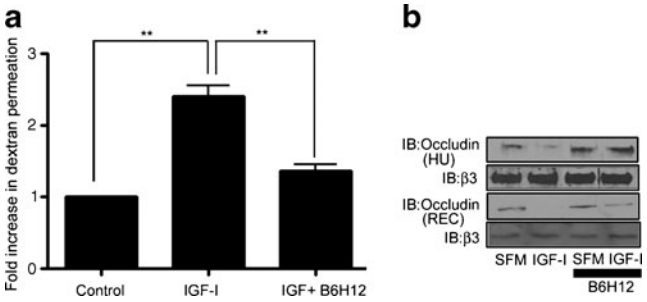

Fig. 2 The association of IAP with SHPS-1 is required for IGF-I-stimulated cell permeability. **a** HUVECs plated on transwell inserts were treated overnight with IGF-I (50 ng/ml) or IGF-I+B6H12 (1 μg/ml), prior to exposure to fluorescently labelled dextran. The mean fold increase in dextran permeation through the membrane (±SEM) is shown; $n=3$; $^{**}p<0.01$ for amount of dextran that permeated in the presence of IGF-I vs control or IGF-I+B6H12. **b** Occludin protein levels were determined by immunoblotting (IB) equal amounts of protein from HUVECs (HU) and RECs treated as described above (**a**). To demonstrate that the difference in occludin levels was not due to a difference in total protein, the lysates were also immunoblotted with an anti-β3 antibody. Bands shown are from discontinuous lanes of the same gel. SFM, SFM-199 medium

IGF-I regulates VEGF production and receptor activation in 15 mmol/l glucose Previous studies have suggested that the response of cells to VEGF is regulated by IGF-I, but it is not known whether this response is altered by hyperglycaemia [17, 18]. In HUVECs, IGF-I stimulated a significant 2±0.5-fold increase (mean±SEM; $n=3$, $p<0.01$) in *VEGF* mRNA. This response was dependent on the association of IAP with SHPS-1, since it was blocked in the presence of B6H12 (Fig. 3a).

To examine the significance of the increase in *VEGF* mRNA, we examined VEGF receptor phosphorylation in HUVECs. IGF-I stimulated a significant 12±9-fold increase (mean ±SEM; $n=3$, $p<0.05$) in VEGF R2 phosphorylation, which was blocked in the presence of B6H12 (Fig. 3b). To determine the significance of this increase, we examined the ability of IGF-I to stimulate a decrease in occludin in the presence of the VEGF inhibitor, Je-11. In the presence of this inhibitor, the IGF-I-stimulated decrease in occludin levels was attenuated (Fig. 3c). We observed a similar response when examining these changes in RECs grown in 15 mmol/l glucose (Fig. 3d, e).

Role of the IAP–SHPS-1 association in vascular permeability in vivo Streptozotocin-induced hyperglycaemia in rats was used to determine whether hyperglycaemia induced an increase in the association of IAP with SHPS-1 in vivo and whether this played a role in the hyperglycaemia-associated increase in vascular permeability.

There was a 2.4±0.6-fold (mean±SEM; $n=9$, $p<0.05$) increase in the association of IAP with SHPS-1 when retinal tissue from hyperglycaemic rats was compared with that from normoglycaemic animals (Fig. 4a). This is somewhat less than the increase in the association of IAP with SHPS-1 observed in cultured endothelial cells in our previous

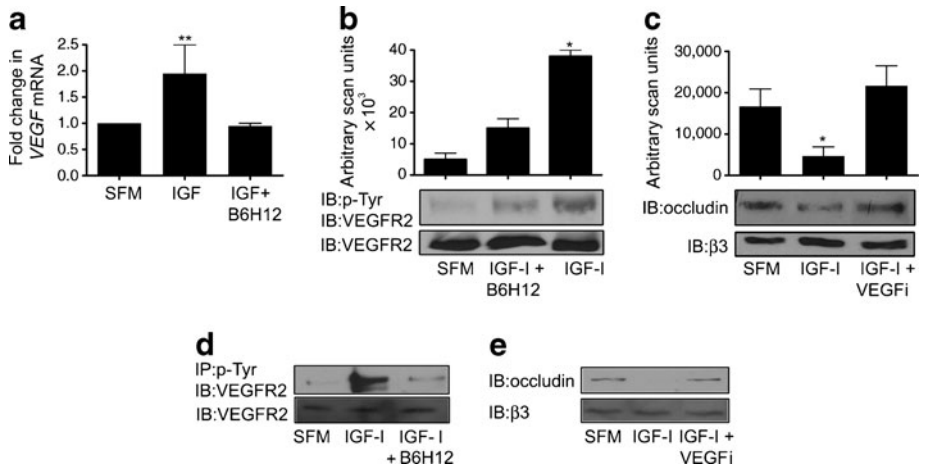

Fig. 3 IGF-I regulates VEGF. **a** RNA was prepared from whole-cell lysates. Total RNA (1 μg) was reverse-transcribed. cDNA (2 μl) was used in each RT-PCR reaction. A standard curve was generated using the control sample (tenfold dilutions from 1 to 10,000). Results of three independent experiments are shown as mean±SEM; $n=3$; $^{**}p<0.01$ for *VEGF* mRNA in the presence of IGF-I vs control (SFM [SFM-199 medium]) or IGF-I+B6H12. **b** HUVECs were grown to confluency in medium containing 15 mmol/l glucose, prior to overnight incubation in serum-free medium with the same glucose concentration plus IGF-I (50 ng/ml), with or without the addition of B6H12 (1 μg/ml). The extent of VEGF receptor 2 (VEGFR2) phosphorylation was determined by immunoprecipitating (IP) with an anti-phosphotyrosine antibody (p-Tyr) and immunoblotting (IB) with an anti-VEGFR2 antibody. To control for differences in protein, cell lysates were also immunoblotted directly with the anti-VEGFR2 antibody. The results of three independent experiments were quantified and expressed as arbitrary scanning units (mean±SEM); $n=3$; $^{*}p<0.05$ for extent of VEGFR2 phosphorylation in the presence of IGF-I vs control (SFM) or IGF-I+B6H12. **c** HUVECs were treated as above (**b**), with or without addition of the VEGF inhibitor (VEGFi) Je-11 (10 μg/ml). Equal amounts of cell lysates were separated by SDS-PAGE and the amount of occludin was assessed by immunoblotting. Quantification is expressed as above (**b**); $^{*}p<0.05$ for the change in occludin in response to IGF-I vs control (SFM) or IGF-I + VEGFi. **d, e** RECs were grown to confluency and treated as HUVECs above (**b**, **c**). Bands shown are from discontinuous lanes of the same gel. Control and IGF-I-treated results are the same as in Fig. 2b

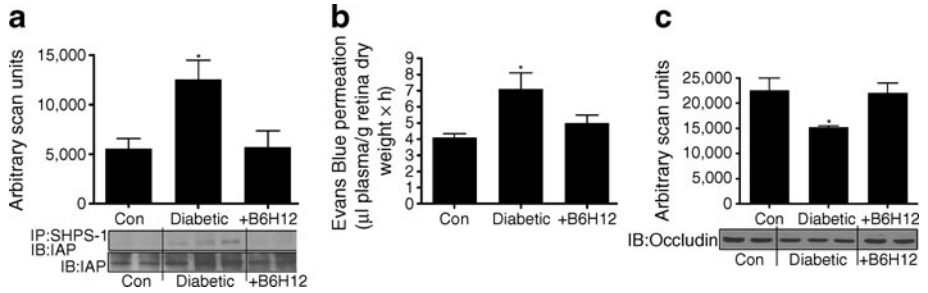

Fig. 4 B6H12 disrupts the association of IAP with SHPS-1 in vivo, thereby inhibiting the diabetes-induced increase of vascular permeability. **a** Individual retinal lysates from control (Con), diabetic and diabetic rats treated with B6H12 (+B6H12) were immunoprecipitated (IP) with an anti-SHPS-1 antibody and immunoblotted (IB) with an anti-IAP antibody, or the lysates were immunoblotted directly with an anti-IAP antibody, R569, that selectively recognises only intact IAP. The association of IAP with SHPS-1 was quantified as arbitrary scanning units given as mean±SEM; $n=9$; *$p<0.05$ for diabetic rats compared with control or diabetic rats treated with B6H12. **b** Evans Blue permeation from the retinal vasculature was measured by spectrophotometry and corrected for plasma concentration, retina weight and time. The amount of Evans Blue from retina from each group of rats is shown (mean±SEM); $n=37$, control non-diabetic; $n=21$, diabetic treated with control IgG; $n=23$, diabetic treated with B6H12. The permeation of Evans Blue from the diabetic retinal vasculature was significantly increased compared with control or diabetic rats treated with B6H12 (*$p<0.05$). **c** Individual retinal lysates from non-diabetic control and diabetic rats treated with control IgG (Diabetic) or with B6H12 (+B6H12) were immunoblotted directly using an anti-occludin antibody. Findings were quantified as arbitrary scanning units, expressed as mean±SEM; $n=9$, *$p<0.05$ for occludin levels in retina from diabetic animals treated with IgG vs control non-diabetic or diabetic animals treated with B6H12

publication [5] and here (Fig. 1a); this difference is probably due to the fact that retinal lysates contain additional cell types compared with pure cultures of endothelial cells. Treatment of hyperglycaemic rats with B6H12 significantly reduced the association of IAP with SHPS-1, such that there was no significant difference between the B6H12-treated rats and control-treated animals (Fig. 4a). Consistent with our in vitro data, we observed a significant increase in the amount of intact IAP in retina from hyperglycaemic rats compared with normoglycaemic control animals. This increase in intact IAP was inhibited in rats treated with B6H12 (Fig. 4a).

Disruption of the association of IAP with SHPS-1 impairs the increase in vascular permeability associated with hyperglycaemia in vivo There was a significant 1.7±0.2-fold (mean±SEM; $n>20$, $p<0.05$) increase in the permeation of Evans Blue from the retinal vasculature of diabetic rats compared with control. Treatment of hyperglycaemic rats with the anti-IAP antibody restored Evans Blue leakage to a level comparable with that of control normoglycaemic rats (Fig. 4b). We also examined occludin levels in normal and diabetic rats. A significant ($p<0.05$) decrease in the amount of occludin was detected in retinal homogenates from hyperglycaemic rats compared with control; however, this was normalised in hyperglycaemic rats treated with B6H12 (Fig. 4c).

Disruption of the association of IAP with SHPS-1 impairs the hyperglycaemia-associated increase in leucocyte adhesion TNFα treatment significantly increased leucocyte adhesion to RECs cultured in 5 and 15 mmol/l glucose. However, significantly more leucocytes adhered to the REC monolayer cultured in 15 mmol/l than to that cultured in 5 mmol/l. Pretreatment of TNFα-stimulated RECs with B6H12 significantly decreased leucocyte adhesion to the REC monolayer (Fig. 5a).

The number of leucocytes adhering to the retinal vasculature in hyperglycaemic rats compared with control was increased significantly (1.4±0.2-fold compared with 2.0±0.3 [mean±SEM]; $p<0.05$). This increase was inhibited in rats treated with B6H12 (1.2±0.2-fold increase; p, NS compared with control) (Fig. 5b).

The role of the IAP–SHPS-1 association in regulating tube formation Neovascularisation, which occurs in diabetes in response to hyperglycaemia, requires cell proliferation, migration and cellular fusion. We have shown previously that the

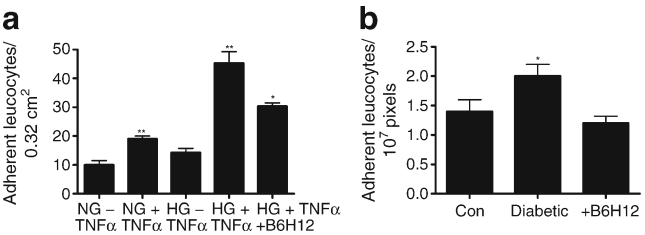

Fig. 5 Disruption of the association of IAP with SHPS-1 disrupts leucocyte adhesion to endothelial cells in hyperglycaemic conditions. **a** The number of fluorescently labelled leucocytes adhering to a confluent monolayer of RECs in normal glucose (NG, 5 mmol/l) or high glucose (HG, 15 mmol/l), in the presence (+) or absence (−) of TNFα with or without B6H12 (1 µg/ml) as indicated was assessed and is expressed as mean±SEM; $n=3$; *$p<0.05$ for leucocyte adhesion in HG+TNFα+ B6H12 vs no B6H12; **$p<0.01$ for leucocyte adhesion in the presence of TNFα vs no TNFα irrespective of glucose culture conditions. **b** Leucocyte adhesion to the retinal vasculature assessed and expressed as number of leucocytes per 10^7 pixels. Values are mean±SEM; $n=14$ (Control [Con]), $n=22$ (Diabetic) and $n=17$ (diabetic + B6H12); *$p<0.05$ for diabetic rats treated with IgG vs non-diabetic or diabetic rats receiving B6H12

hyperglycaemia-induced increase in IAP–SHPS-1 is required for the increased proliferation of RECs in response to IGF-1 [5]. To extend those observations, we analysed the role of IAP–SHPS-1 formation in in vitro tube formation in HUVECs in response to IGF-I. A representative image and quantification of three independent experiments is shown in Fig. 6a, b. In the presence of IGF-I, there was a significant (32.9±2.61-fold [mean±SEM; n=3]) increase in the number of tubes formed (Fig. 6b). In contrast, in the presence of B6H12, the number of tubes formed was reduced significantly and not different from that in control cultures. The ability of IGF-I to stimulate an increase in tube formation was not altered in the presence of the VEGF inhibitor (Fig. 6c, d).

Disruption of the association of IAP with SHPS-1 impairs neoangiogenesis in a rodent model of hypoxic retinopathy Currently, there are no rodent models in which diabetes-accelerated neovascularisation is comparable to that seen in human patients with diabetes. However, the rodent model of retinopathy of prematurity (ROP) used here allows testing of anti-angiogenic strategies in vivo. We first compared the level of IAP in retinal homogenates from rat pups exposed to room air with that from ROP rat pups. There was a significant increase in the amount of intact IAP, and correspondingly a decrease in the IAP fragment in ROP pups compared with control (Fig. 6e). We then tested the ability of B6H12 to impair the IVNV that occurs in ROP rats. In room air pups, retinal vascularisation of the inner capillary plexus extends to the ora serrata and there is no avascular retina or IVNV. In ROP pups, avascular retina is 30% of the total retinal area at p14 and 25% at p18. Approximately four clock hours of IVNV were present at p18 (Fig. 6f). Treatment with B6H12 markedly reduced the number of clock hours exhibiting IVNV (from 4.1±0.4 to

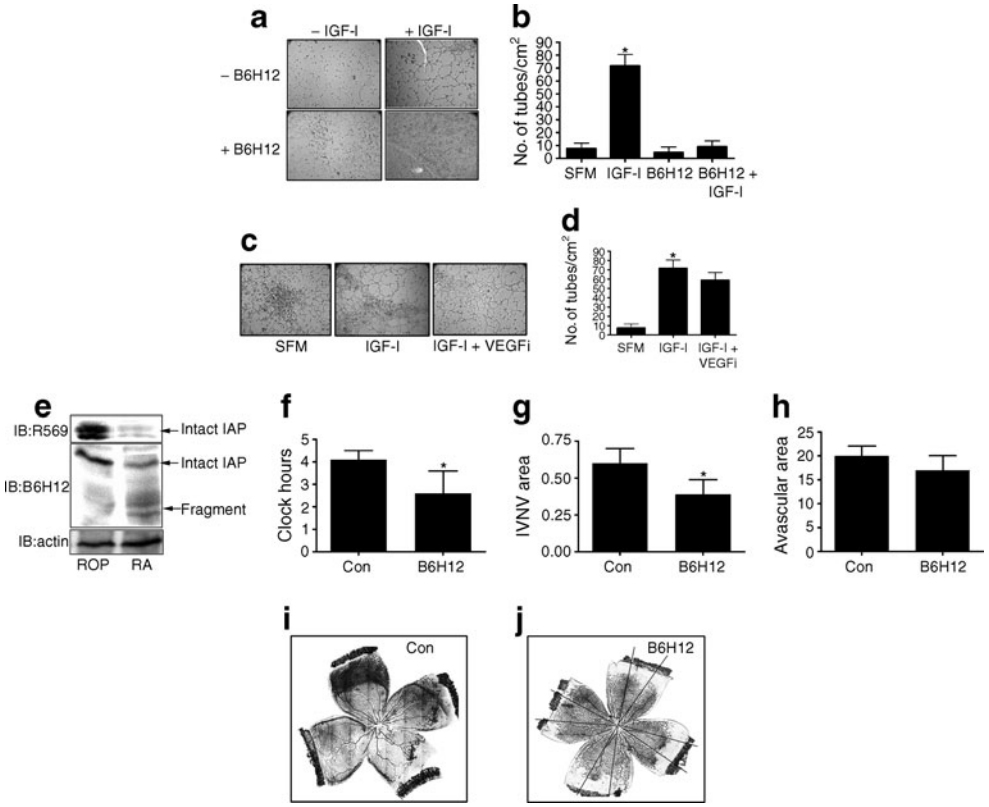

Fig. 6 Disruption of the association of IAP with SHPS-1 impairs IVNV in a rodent model of ROP. **a** HUVECs were plated on growth factor-reduced matrigel in the presence (+) or absence (−) of IGF-I (50 ng/ml), and/or B6H12 (1 μg/ml), and tube formation was allowed to proceed for 4 h, at which point photographs were taken at magnification ×10. The tube number was quantified (**b**) and is expressed as mean±SEM from three independent experiments. SFM, SFM-199 medium. The three crosses indicate two tubes (1, 2) originating from a single branch point (**a**). **c** HUVECs were treated as above (**a**), but with or without VEGF inhibitor (VEFGi, 10 μg/ml) as indicated, and tube formation quantified and documented as above (**a**). **d** Quantification of tube number, expressed as mean±SEM from three independent experiments. **b**, **d** n=3; *p<0.05 for number of tubes in the presence of IGF-I vs that formed in SFM alone or in the presence of IGF-I + B6H12 or IGF-I + VEGFi. **e** Pools of retinal lysates from room air (RA) and ROP rat pups were immunoblotted (IB) with an anti-IAP antibody that specifically recognises intact IAP R569 or with anti-IAP antibody B6H12, which specifically recognises intact and fragmented IAP. An actin immunoblot is shown as a loading control. **f–h** Lectin-stained retinal flat mounts from pups injected at p12 with B6H12 or control IgG (Con) were analysed at day 18 and the number of clock hours of IVNV, total IVNV area and avascular area was calculated *p<0.05 for control (Con) vs B6H12. **i** Representative images of control and (**j**) B6H12-treated retinal flat mounts

2.0±1.0 [mean±SEM]; $p<0.05$), as well as the total IVNV area (from 0.6±0.1% of total area to 0.39±0.1%; $p<0.05$) (Fig. 6f, g). No significant difference was observed in the amount of avascular area when untreated ROP animals were compared with ROP animals treated with B6H12 (Fig. 6h).

Discussion

The results of this study show that an increase in intact IAP and an increase in its association with SHPS-1 is a generalised endothelial cell response to hypeglycaemia, and is required (1) for the endothelial tube formation and increased endothelial permeability that occur in response to IGF-I during hyperglycaemia, as well as (2) for glucose-enhanced leucocyte adherence to endothelial cells. Culture of cells in normal glucose led to proteolytic cleavage of the region of IAP that contains the SHPS-1 binding site, resulting in loss of IAP–SHPS-1 association and of the ability of IGF-I to stimulate SHPS-1 phosphorylation and downstream signalling. In contrast, exposure to 15 mmol/l glucose protected IAP from cleavage, allowing SHPS-1 to associate with IAP and also allowing IGF-I-stimulated SHPS-1 phosphorylation. The significance of these in vitro findings is that not only was there an increase in the association of IAP with SHPS-1 in retinal homogenates from diabetic rats, but that blocking this increase inhibited the pathophysiological changes that have been identified during the early stages of diabetic retinopathy, e.g. increased endothelial permeability and leucocyte adherence [19, 20]. These results strongly suggest that the increase in SHPS-1–IAP association may be a critical step in the biochemical events leading to these early changes in the endothelium in response to hyperglycaemic stress.

Several studies have linked IGF-I to stimulation of diabetic retinopathy [1–4]. Endothelial cells in culture have been shown to secrete increased amounts of IGF-I in response to hyperglycaemia [21, 22]. Transgenic overexpression of *Igf1* in mice has been associated with several changes in the retina that occur in diabetic retinopathy, including loss of pericytes, thickening of the capillary basement membrane and neovascularisation [4]. Administration of IGF-I to patients with diabetes has been associated with the development of retinal oedema, with some evidence of increased retinopathy progression [23]. Similarly, administration of octreotide decreases IGF-I levels in vitreous and slows retinopathy progression [3]. Our findings suggest that inhibition of IGF-I signalling by disruption of the association of IAP with SHPS-1 represents a potentially effective treatment strategy.

Our data suggest a direct, but complex relationship between IGF-I and VEGF in mediating the changes that occur in the diabetic retina. One previous study clearly indicated that IGF-I stimulates VEGF synthesis during angiogenesis in the rodent model of ROP [17]. Our data indicate that during hyperglycaemic conditions IGF-I can induce VEGF synthesis and secretion, resulting in VEGF receptor activation. We did not address the question of whether the ability of IGF-I to stimulate VEGF actually requires hyperglycaemic stress, but previous studies have suggested this possibility [24]. VEGF is a stimulant of angiogenesis, and inhibition of its receptor in diabetes has been shown to be anti-angiogenic and to inhibit retinal capillary leakage of proteins [25, 26]. In our studies, we showed that IGF-I can support angiogenesis in a VEGF-independent manner, suggesting that IGF-I may contribute to the proliferative phase of diabetic retinopathy both directly, by stimulating angiogenesis, and indirectly by increasing VEGF production. In contrast to the VEGF-independent effects of IGF-I on tube formation, the ability of IGF-I to stimulate a decrease in occludin and thus increase vascular permeability was dependent on VEGF-mediated signalling, since it was blocked in the presence of the VEGF inhibitor.

Several junctional proteins have been linked to changes in permeability in retinal endothelium. These include claudin-5, zonula occludens protein 1 (ZO1), vascular endothelial cadherin (VE cadherin) and occludin [27]. Occludin binds within the tight junctions to the Src homology 3 guanylate kinase (SH3-GUK) homology domain of ZO1 [28]. Disassociation from the cell border and lower concentrations of total occludin occur in diabetes [29]. Exposure to VEGF also stimulates these changes, and VE cadherin also undergoes phosphorylation and internalisation in response to VEGF stimulation [29]. The VE cadherin content is decreased in vessels of diabetic rats, and its concentration correlates inversely with vascular permeability [30]. Decreased association of VE cadherin with β-catenin also occurs in diabetic vessels. These changes are believed to be due primarily to changes in VE cadherin and β-catenin phosphorylation [28]. Protein kinase C isoforms and proto-oncogene Src (c-SRC) have been shown to phosphorylate the above substrates, leading to altered vascular permeability. SRC phosphorylation of occludin leads to its disassociation from the adherens complex and its degradation [30]. VEGF has been shown to stimulate SRC-dependent occludin phosphorylation and SRC can also phosphorylate ZO1, leading to changes in its localisation [31]. Since IGF-I-stimulated SHPS-1 phosphorylation in vascular smooth muscle cells enhances SRC activation, this represents a potential mechanism leading to occludin downregulation in response to hyperglycaemia [32, 33]. Future studies will be required to determine whether stimulation of IGF-I signalling has direct effects on the localisation of VE cadherin, β-catenin or other components of endothelial cell tight junctions and/or an effect mediated through its regulation of VEGF signalling.

The translational impact of these observations is hard to predict. The duration of diabetes in the rodents studied was very short compared with the time needed for diabetic

retinopathy to develop in humans. While the severity of retinopathy in animal models increases with duration of diabetes, it remains mild compared with that seen in many patients with diabetes. In addition, our studies focused on endothelial cells, but the development of diabetic retinopathy includes changes in other cell types such as pericytes and retinal pigmented epithelial cells.

Despite these limitations, and taken together with our other recent study [5], our data indicate that the hyperglycaemia-induced increase in the association of IAP with SHPS-1 is a generalised response of endothelial cells and one that contributes to changes in endothelial cell function. Our data also suggest that this novel biochemical pathway may contribute to the early changes in vascular cell function that occur in diabetes, including those linked to diabetic retinopathy.

Acknowledgements The authors wish to thank L. Lindsey (University of North Carolina at Chapel Hill) for her help in preparing the manuscript.

Duality of interest The authors declare that there is no duality of interest associated with this manuscript.

Contribution statement All authors were involved in the conception and design, analysis and interpretation of data. All authors contributed to the drafting or revising of the article, and all authors gave final approval of the version to be published.

Funding This work was supported by a grant from the Juvenile Diabetes Research Foundation (17-2008-1048).

References

1. Merimee TJ, Zapf J, Froesch ER (1983) Insulin-like growth factors. Studies in diabetics with and without retinopathy. N Engl Med 309:527–530
2. Meyer-Schwickerath R (1993) Vitreous levels of the insulin-like growth factors I and II, and the insulin-like growth factor binding proteins 2 and 3, increase in neovascular eye disease. Studies in nondiabetic and diabetic subjects. J Clin Invest 92:2620–2625
3. Grant MB, Mames RN, Fitzgerald C et al (2000) The efficacy of octreotide in the therapy of severe nonproliferative and early proliferative diabetic retinopathy. Diabetes Care 23:504–509
4. Ruberte J, Ayuso E, Navarro M et al (2004) Increase in ocular levels of IGF-I in transgenic mice lead to diabetes-like eye disease. J Clin Invest 113:1149–1157
5. Miller E, Capps BE, Sanghani R, Clemmons DR, Maile L (2007) Regulation of IGF-I signaling in retinal endothelial cells by hyperglycemia. Invest Opthalmol Vis Sci 48:3878–3887
6. Maile LA, Capps BE, Ling Y, Xi G, Clemmons DR (2007) Hyperglycemia alters the responsiveness of smooth muscle cells to insulin-like growth factor-I. Endocrinology 148:2435–2443
7. Maile LA, Capps BE, Miller E et al (2008) Glucose regulation of integrin-associated protein cleavage controls the response of vascular smooth muscle cells to insulin-like growth factor-I. Mol Endocrinol 22:1226–1237
8. Maile LA, Badley-Clarke J, Clemmons DR (2003) The association between integrin-associated protein and SHPS-1 regulates insulin-like growth factor-I receptor signaling in vascular smooth muscle cells. Mol Biol Cell 14:3519–3528
9. Arnaoutova I, Kleinman HK (2010) In vitro angiogenesis: endothelial cell tube formation on gelled basement membrane extract. Nat Protoc 5:628–635
10. Xu Q, Qaum T, Adamis AP (2001) Sensitive blood–retinal barrier breakdown quantitation using Evans blue. Invest Ophthalmol Vis Sci 42:789–794
11. Penn JS, Henry MM, Wall PT, Tolman BL (1995) The range of PaO_2 variation determines the severity of oxygen induced retinopathy in newborn rats. Invest Ophthalmol Vis Sci 36: 2063–2070
12. Chan-Ling T (1997) Glial, vascular and neuronal cytogenesis in whole-mounted cat retina. Microsc Res Tech 36:1–16
13. Budd SJ, Thompson H, Hartnett ME (2009) Reduction in endothelial tip cell filopedia corresponds to reduced intravitreous but not intraretinal vascularization in a model of ROP. Exp Eye Res 89:718–727
14. Hartnett ME, Mariniuk DJ, Saito Y, Geisen P, Peterson LJ, McColm JR (2006) Triamcinolone reduces neovascularization, capillary density and IGF-I receptor phosphorylation in a model of oxygen-induced retinopathy. Invest Opthalmol Vis Sci 47:4975–4982
15. Geisen P, Peterson LJ, Martiniuk D, Uppal A, Saito Y, Hartnett ME (2009) Neutralizing antibody to VEGF reduces intravitreous neovascularization and may not interfere with ongoing intraretinal vascularization in a rat model of retinopathy of prematurity. Mol Vis 14:345–357
16. Werdich XQ, Penn JS (2006) Specific involvement of Src family kinase activation in the pathogenesis of retinal neovascularization. Invest Opthalmol Vis Sci 47:5047–5056
17. Punglia RS, Lu M, Hsu J et al (1997) Regulation of vascular endothelial growth factor expression by insulin-like growth factor-I. Diabetes 46:1619–1626
18. Smith LE, Shen W, Peruzzi C et al (1999) Regulation of vascular endothelial growth factor-dependent neovascularization by insulin-like growth factor-1 receptor. Nat Med 5:1390–1395
19. Xu X, Zhu Q, Xia S, Zhang S, Gu Q, Luo D (2004) Blood-retinal barrier breakdown induced by activation of protein kinase C via vascular endothelial growth factor in streptozocin-induced diabetic rats. Curr Eye Res 28:251–256
20. Berkowitz BA, Roberts R, Luan H, Peysakhov J, Mao X, Thomas KA (2004) Dynamic contrast-enhanced MRI measurements of passive permeability through blood retinal barrier in diabetic rats. Invest Opthalmol Vis Sci 45:2391–2398
21. Spoerri P, Ellis E, Tarnuzzer R, Grant M (1998) Insulin-like growth factor: receptor and binding proteins in human retinal endothelial cell cultures of diabetic and non-diabetic origin. Growth Horm IGF Res 8:125–132
22. Spraul CW, Baldysiak-Figiel A, Lang GK, Lang GE (2002) Octreotide inhibits growth factor-induced bovine choriocapillary endothelial cells in vitro. Graefes Arch Clin Exp Ophthalmol 240:227–231
23. Kolaczynski JW, Caro JF (1994) Insulin-like growth factor-I therapy in diabetes: physiologic basis, clinical benefits and risks. Ann Intern Med 120:47–55
24. Treins C, Giorgett-Peraldi S, Murdaca J, Monthouel-Kartmann MN, van Obberghen E (2005) Regulation of hypoxia-inducible factor (HIF)-1 activity and expression of HIF hydroxylases in response to insulin-like growth factor I. Mol Endocrinol 19: 1304–1317
25. Avery RL, Pearlman J, Piermici DJ et al (2006) Intravitreal bevacizumab (Avastin) in the treatment of proliferative diabetic retinopathy. Opthal 113:1695.e1-15
26. Ideno J, Mizukami H, Kakehashi A et al (2007) Prevention of diabetic retinopathy by intraocular soluble ft1 gene transfer in a spontaneously diabetic rat model. Int J Mol Med 19: 75–79

27. Bucolo C, Ward KW, Mazzon E, Cuzzocrea S, Drago F (2009) Protective effects of a coumarin derivative in diabetic rats. Invest Opthalmol Vis Sci 50:3846–3852
28. Steed E, Balda M, Matter K (2010) Dynamics and functions of tight junctions. Trends Cell Biol 3:142–149
29. Leal EC, Martins J, Voabil P et al (2010) Calcium dobesilate inhibits the alterations in tight junction proteins and leukocyte adhesion to retinal endothelial cells induced by diabetes. Diabetes 59:2637–2645
30. Dejana E, Orsenigo F, Lampugnani M (2008) The role of adherens junctions and VE-cadherin in the control of vascular permeability. J Cell Sci 121:2115–2122
31. Elias BC, Suzuki T, Seth A et al (2009) Phosphorylation of Tyr-398 and Tyr-402 in occludin prevents its interaction with ZO-1 and destabilizes its assembly at the tight junctions. J Biol Chem 284:1559–1569
32. Murakami T, Felinski EA, Antonetti DA (2009) Occludin phosphorylation and ubiquitination regulate tight junction trafficking and vascular endothelial growth factor-induced permeability. J Biol Chem 284:21036–21046
33. Shen X, Xi G, Radhakrishnan Clemmons DR (2010) Recruitment of Pyk2 to SHPS-1 signaling complex is required for IGF-I-dependent mitogenic signaling in vascular smooth muscle cells. Cell Mol Life Sci 67:3893–3903